Relationships among Sea Surface Temperature, Sea Surface Height and Volume Transport in Makassar Strait

張, 甘夢
九州大学大学院総合理工学府大気海洋環境システム学専攻

出版情報：Kyushu University, 2021, 修士, 修士
バージョン：

Relationships among Sea Surface Temperature, Sea Surface Height and Volume Transport in Makassar Strait

ZHANG GANMENG

Supervisor: Kaoru Ichikawa

Abstract

The Makassar Strait through flow is one of the Indonesian passage currents from the Pacific Ocean to the Indian Ocean. It is well known that sea surface height (SSH) reflects the heat capacity of the surface. Meanwhile, SSH is also related with heat content of the surface layer; in ENSO events, SSH is known well correlated with sea surface temperature (SST). Therefore, this study uses the data of satellite sea surface height and sea surface temperature (SST) in the Makassar Strait to investigate the correlation between the time changes. SST and SSH vary independently for annual cycles, but they show good correlation for sub-seasonal cycles. Propagations of these baroclinic sub-seasonal variations in the Strait are further studied by high-density SST field.

Contents

1.Introduction

Makassar Strait is the strait between Borneo Island and Sulawesi Island in Indonesia (Fig.1.1). It is about 800 km long and 250 km wide on average, connecting the Celebes Sea to the north, Java Sea and Flores sea to the south. It's the inland sea of Indonesia. Important ports on both sides of the Strait include Balikpapan, Makassar, etc. In the northeast, it forms the Sangkulirang Bay in the south of Mangkalihat Peninsula. The Strait is an important regional shipping channel in Southeast Asia. The Mahakam Rive and Karangan River of Borneo flow into the Strait. Ports along the Strait include Balikpapan and Bontang in Borneo, and Makassar, Palu and Parepare in Sulawesi. The city of Samarinda is 48 kilometers (30 miles) from the Makassar Strait.

Fig.1.1 Geographical location of Makassar Strait.
The red line is the equator.
(Map source: Google Earth, 2021）

The complex basins and watercourses of marine continents (including the Indonesian sea) constitute the only exchange channel between tropical oceans in the world. They provide a conduit for the Pacific Ocean to enter the Indian Ocean, forming a key component of the larger scale ocean and climate system. Makassar channel, with a bottom depth of 680 m, is the westernmost channel of Indonesian throughflow

(ITF). The Makassar Strait flows into the Lombok Strait through the current channel of the North Pacific and into the Banda Sea through the Flores sea. The Makassar Strait throughflow flows through the eastern passage of the Molucca Sea and the Halmahera Sea, and draws water from the South China Sea through the Karimata Strait. The eastern passage mainly takes water from the South Pacific Ocean, and undergoes a sub temporary mixing driven by strong tidal dissipation, which significantly changes the thermohaline stratification profile in the Banda Sea, and then exports to the Indian Ocean.

Among the tropical oceans, only the Indian Ocean and the Pacific Ocean are directly connected geographically. Makassar Strait, as an important passage from the Western Pacific to the Indian Ocean, is of great significance to the research of Marine Physics in the Strait.

Makassar Strait is dominated by annual variation (monsoon), and the difference between dry and wet seasons plus the interannual climate event ENSO / IOD. Due to these multi-scale properties, the variations in the Strait are complex.

El Nino/Southern Oscillation abbreviated as ENSO, is a climate event. ENSO is an El Nino with abnormal warming of sea surface temperature in the equatorial Middle East Pacific Ocean. The event and the southern oscillation phenomenon of the interannual variation of the tropical Pacific atmospheric circulation. Bjerknes first discovered the close relationship between El Nino event and Southern Oscillation in 1969 (Bjerknes, 1969), and then put forward the concept to express the air sea interaction in the tropical Pacific. The warm phase of ENSO event is El Nino. The results show that the sea surface temperature in the Middle East Pacific is abnormally high, the thermocline is abnormally deep, the sea level pressure is decreased and the rainfall is increased, while the air sea anomaly in the West Pacific is opposite; The cold phase is La Nina. Performance and El Nino events are the opposite. The warm and cold phases constitute an irregular cycle of 2 to 7 years, also known as ENSO cycle.

There are many views on the cause of ENSO formation in the scientific community. The common view is that under normal conditions, northeast trade wind blows near the equator of the northern hemisphere and southeast trade wind blows near the equator of the southern hemisphere. The trade wind drives the sea water to flow from east to west, forming the North Equatorial current and the South Equatorial warm current respectively. The sea water flowing from the equatorial east Pacific Ocean is supplemented by upwelling current at the bottom of the ocean. Due to the lower temperature of the bottom water, the surface water temperature is lower than that around, resulting in the temperature difference between the East and the West. However, once the east wind weakens or even turns into the west wind, the cold water in the equatorial eastern Pacific region will turn up, decrease or stop, and the sea water temperature will rise, forming a large range of abnormal warming of sea water temperature.

In 1999, scientists such as Saji et al., (1999) first discovered that the Indian Ocean also has an interannual variation that is similar to ENSO from the air sea observation data in the past 40 years, namely IOD. IOD usually appears in the northern hemisphere summer, and reaches its peak in September to November, then disappears, with the characteristics of seasonal lock-in. Similarly, IOD also has positive and negative phases: during the positive phase, the sea water in the Sumatra Java coast of the tropical southeast Indian Ocean becomes abnormally cold and the rainfall decreases, while the sea surface temperature in the West Indian Ocean increases abnormally and the rainfall increases along the coast of East Africa; In the negative phase, on the contrary, the sea surface temperature of the East Indian Ocean increased abnormally and the rainfall increased; And the West Indian Ocean is getting colder and less rainfall. Negative IOD events usually occur in the following year when positive IOD events occur, and there is a quasi-biennial-cycle in the positive and negative phases (Saji et al., 1999; Rao et al., 2002).

As an important interannual variation signal of the coupled system, the interaction and interaction between IOD and ENSO has been widely concerned by scientists. Generally speaking, positive IOD events are usually associated with El Nino events occur simultaneously, while negative IOD events are associated with La Nina event occurred simultaneously (Wang et al., 2004; Annamarai et al., 2005; Behra et al., 2006; Luo et al., 2010).

The research supporting the atmospheric bridge hypothesis suggests that the abnormal increase / decrease of sea surface temperature in the East Indian Ocean during IOD can cause the increase / decrease of Walker circulation, thus causing the East / west wind anomaly in the equatorial western Pacific, which has an impact on the development of ENSO in the Pacific.

In recent years, the research shows that as a geographical channel connecting the Indian Ocean and the Pacific Ocean, the role of ocean would not be ignored in the process of the influence of the IOD one year ahead of the ENSO. Yuan et al. (2011) conducted a series of experiments using reduced gravity model, ocean circulation model and sea air coupling model respectively. It is proved that IOD can influence ENSO by changing the annual change of ITF flow. During positive IOD, the East Indian Ocean sea water becomes cold, sea level decreases, pressure gradient from Pacific to Indian Ocean increases, and ITF flow increases, Thus, more heat will be transferred from the equatorial Pacific to the Indian Ocean; This will lead to the rise of the temperature jump layer in the western equatorial Pacific and the abnormal decrease of the subsurface sea temperature.

Based on previous studies Napitu et al. (2018) identified and analyzed the physical processes that regulate the variation of surface ITF, especially those that vary on a seasonal time scale, inferred from observations in the Makassar Strait from January 2004 to August 2011 and from August 2013 to December 2016. December, January, February and March were classified as DJFM; June, July, August and September are classified as JJAS. The observation confirmed the existence of the southern monsoon, the seasonal circulation driven by the surface to Nantong current, and the minimum (maximum) transmission occurred during DJFM (JJAS). The decrease of surface ITF transmission during DJFM is not only attributed to monsoon, but also affected by seasonal events. During the DJFM period, the transport anomalies in the surface layer obviously show a change of 1 to 3 months.

Sea surface height (SSH) is caused by astronomical and non astronomical forces. It has periodic modulation based on astronomical interaction, such as moon earth, moon day and so on. There are also some non astronomical phenomena that affect the sea surface height, such as monsoon, El Nino Southern Oscillation and so on. The sea surface can change its height according to the force acting on the whole water area.

According to the research results of Radjawane and Azminuddin (2016), the monthly variation of mean sea height anomaly (SSHA) increases from the north to the south of the Strait. During the 9-14 months affected by monsoon system, SSHA was dominant. During the northwest monsoon, SSHA increases by about 3 to 9 cm, reaching its maximum in February in the southern part of the Strait. Semiannual variation is also detected in the signal period of 5-7 months, which usually occurs during the transitional monsoon period of April / May and November / December. This phenomenon is related to the propagation of Kelvin wave from Lombok Strait to Makassar Strait.

According to the previous research of Pujina et al. (2019), the sea level difference in the Pacific Ocean is set as ηN, and the sea level difference in the Indian Ocean is set as ηS (Fig.3.1). Through the study of Pujina et al. (2019), it can be concluded that when the sea level on the Pacific side is high and the sea level on the Indian side is low, the traffic volume is negative, indicating that the pressure is the driving force of the through flow.

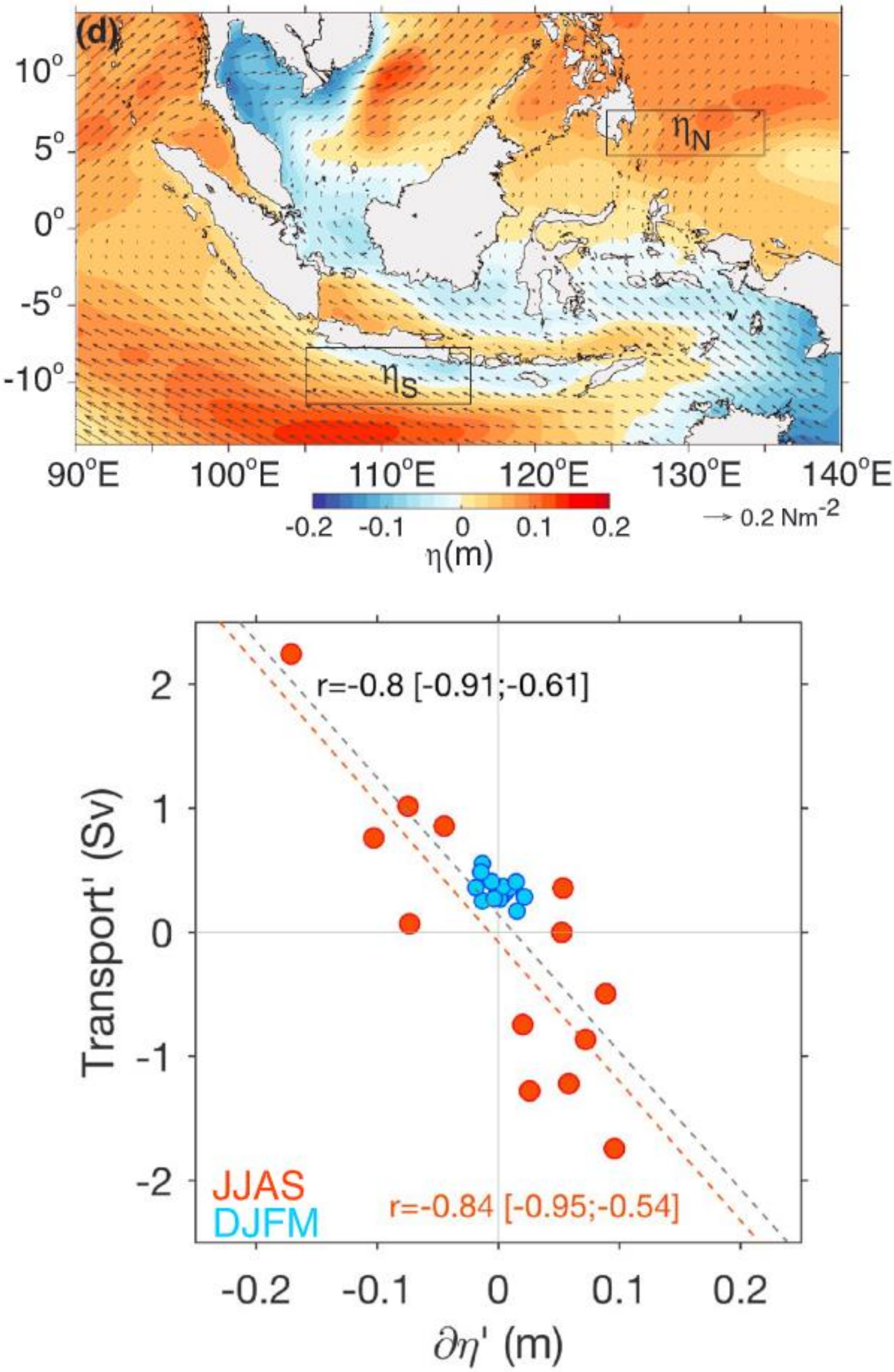

Fig.1.2 Location of ηS and ηN (up)

Scatter figure of sea level difference and transport (down)

From Pujina et al. (2019)

Pujina et al. (2019) studied the relationship between volume transport and SSH, and the change of ITF in Makassar Strait during climate anomalies. But because the satellite altimeter data is close to the island and land, it has very low reliability. If the satellite altimeter has land in a footprint (about 10 km), the observation results will be polluted. Therefore, previous studies avoided using satellite altimeter SSH data in the Strait. Pujina et al. (2019) used SSH data from the Pacific Ocean and Indian Ocean to obtain SSH data in the Strait based on spatial interpolation.

Recently, however, a new algorithm was developed by Wang et al. (2019). With the support of the new algorithm, made us allowed to use satellite altimeter SSH data near land or island for research.

We are treating SSH, SST, VT all of which would be related each other, in a certain condition:

1. VT = Velocity = Pressure gradient = SSH gradient; may be out of phase with SSH at some events.
2. SST = surface temperature = related with baroclinic SSH change (variation of the thermocline depth); may be out of phase with barotropic SSH (height change without thermocline depth variations, such as piling up of the Ekman layer water).

Therefore, due to the small Coriolis parameter in tropical area, SSH is used as the index of surface heat content. Through the compare of SSH with SST and volume transport (VT), to discuss the relationship between sea surface heat content, temperature and horizontal heat flux. And by comparing SSH and SST in Makassar Strait, the study about how they respond to multi-scale variations will be discussed.

This paper focuses on the relationship among SSH, SST and VT in the Makassar Strait during the climate events (ENSO and IOD). It also discusses the influence of seasonal factors on the relationship among SSH, SST and VT, and discusses the relationship among SSH, SST and VT in the sub-seasonal after eliminating the seasonal factors.

The specific chapters of this paper are as follows:

Chapter 1: introduces the natural conditions of the study area and the main climate abnormal events studied in this paper.

Chapter 2: introduces the data sources, the characteristics of satellite data and the data processing methods.

Chapter 3: the relationship among SSHA, SSTA and VTA, including their relationship in annual cycle and sub seasonal variation, will be studied.

Chapter 4: the reliability of the results will be discussed and the propagations of sub-seasonal variations in Makassar Strait will be additional analyzed.

Chapter 5: summarize the research work of this paper, discuss the results and prospects for future research.

2. Materials and Methods

2.1 Data sources

2.1.1 SSH data

SSH data in this study is extracted from Jason-2 satellite Pass114.

The ocean surface topography task on the Jason-2 satellite (OSTM/Jason-2) is the follow-up task of JASON-1. It was launched from Vandenberg Air Force Base in California on June 20, 2008. Jason 2 is a global satellite designed to observe Ocean Topography to investigate the rise of sea level and the relationship between ocean circulation and climate change. The satellite also provides data on the forces behind large-scale climate phenomena such as El Nino and La Nina. Due to the scope of the study channel area, the SSH data used in this paper are from Jason-2 Pass114 orbit (Fig.2.1), with a data of 20Hz and a period from July 2008 to December 2016. Processed by Wang et al., (2019), for coastal research purposes.

2.1.2 SST data

The heat, momentum and freshwater flux on the surface of the sea are the basic physical quantities, which are essential to understand the sea air interaction and the nature of the climate system. In order to understand the behavior of these fluctuations in the context of climate change, it is necessary to quantitatively and observe the surface fluxes in a wide range of regions and in the long term. Because the time or space coverage of in-situ observation platforms such as ships and surface buoys are very limited, it is difficult to use their data only to evaluate the global surface flux. Satellite remote sensing technology can better cover large area of longer time period with higher time and spatial resolution.

J-OFURO3 is the 3rd generation data set developed by the Japanese ocean flux data set using the J-OFURO research project. It represents a significant improvement on the old data set, because of the results of research and development from multiple perspectives. J-OFURO3 provides a data set of surface heat, momentum, freshwater flux and related parameters for the global ocean (except sea ice areas) from 1988 to 2013. The surface flux data is based on 0.25 degrees grid system, which has higher spatial resolution and is more accurate than previous efforts. This is achieved by using the most advanced algorithm to estimate the specific humidity of near surface air and the observation improvement technology using multi satellite sensors. The system developed with J-

OFURO3 data set is compared with in situ observation, which proves that accuracy is improved, and the comparison with other data sets is also true.

The SST data in this study is from J-OFURO3 (Tomita et al., 2019), using daily SST data and interpolating to 0.06 ° grid (Fig.2.1).

2.1.3 VT data

According to the research of Gordon et al. (2018), at the end of 1996, as a part of Arlindo circulation plan, two mooring equipment were deployed in the restricted area of Makassar Strait, namely, the Rabbani strait with a width of 45 km (50 m deep), and the ITF was recorded until the middle of 1998 (Ffield et al., 2000; Gordon et al., 1999; Susanto & Gordon, 2005). In 2004, the Labani Strait mooring facility was first redeployed as part of the international Nusantara stratification and transportation program (install) 2004-2006 (Gordon et al., 2008, 2010) to monitor multiple ITF routes simultaneously. After the termination of the install program in December 2006, Labani channel time series continued to be used as a monitoring ITF (MITF); Gordon et al., 2012; Susanto et al., 2012), which has been maintained until now. The last one was mooring recovery and data download in August 2017, and it was re deployed in November 2017.

VT in this paper is the upper layer data, which comes from the research of Gordon et al. (2018). The VT definition points can be seen in Fig.2.1. The X symbol in the Makassar Strait marks the current measured mooring position in the Rabbani Strait: 2 ° 51′S, 118 ° 28 ′ E, water depth 2137 m. Note that all VT values are negative, i.e., southward in the study period.

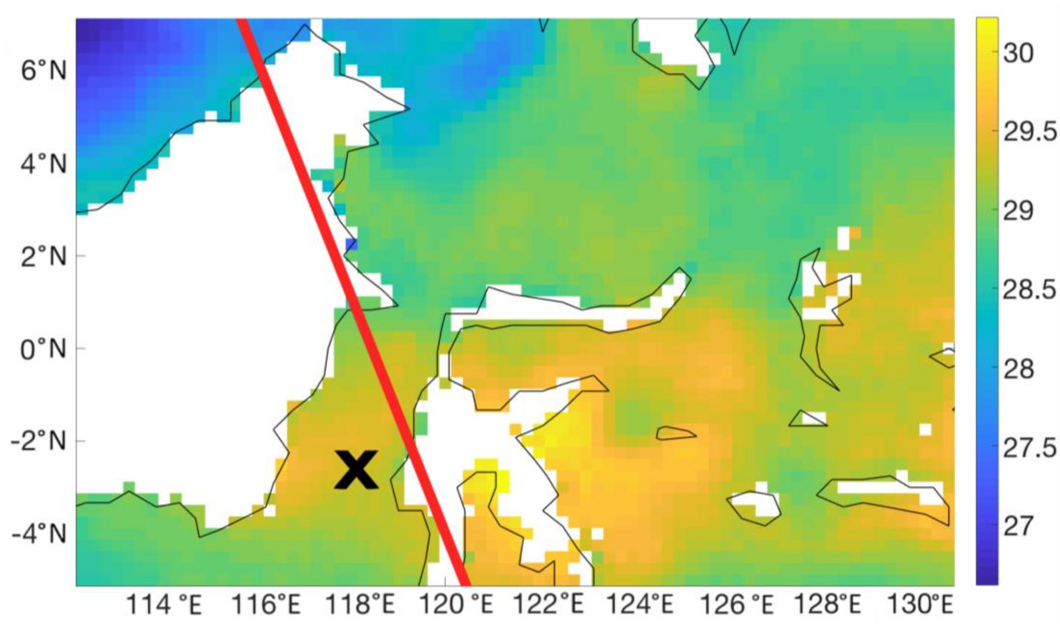

Fig.2.1 Example of monthly average SST (deg C) in research area. The red line is the Jason-2 track. Location of measurement point of VT is indicated by X mark

2.1.4 ENSO and IOD index

According to the climate data provided by Japan Meteorological Agency, we defined the cycle of ENSO and IOD. The ENSO and IOD cycles we defined are shown in the table below.

El Nino	La Nina	IOD+	IOD-
2009/6-12	2010/7-12	2008/6-8	2010/8-11
2010/1-3	2011/1-3	2011/8-10	2013/4-9
2014/6-12		2012/7-10	2016/6-11
2015/1-12		2015/8-11	
2016/1-4			

2.2 Data processing

2.2.1 Along track processing

Because the SSH data comes from Jason-2 Pass114 along track data, Wang et al. (2019) averaged the SSH data 35 km along the track. SST data are also extracted along the orbit according to Jason-2 SSH data.

2.2.2 Anomaly calculation

In order to describe the variation of sea surface height, sea surface temperature and volume transport more accurately, this paper introduces the calculation of anomaly. Remove the mean value of Jason-2 from each SSH data to get the anomaly value of sea surface height, which is called SSHA.

SST and VT are also calculated using the same anomaly calculation to obtain SSTA and VTA. By calculating anomaly, we can get the time series figures of SSHA, SSTA and VTA (Fig.2.2)

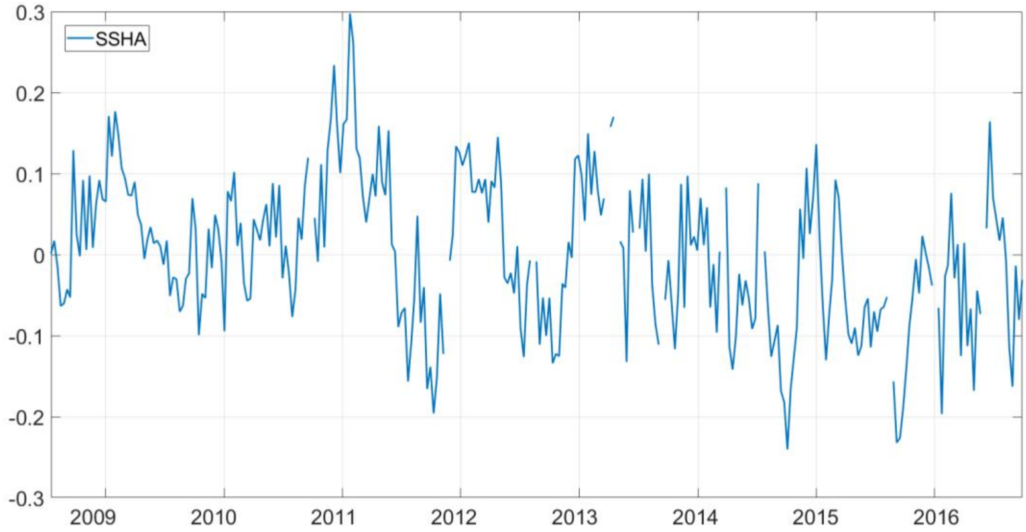

a

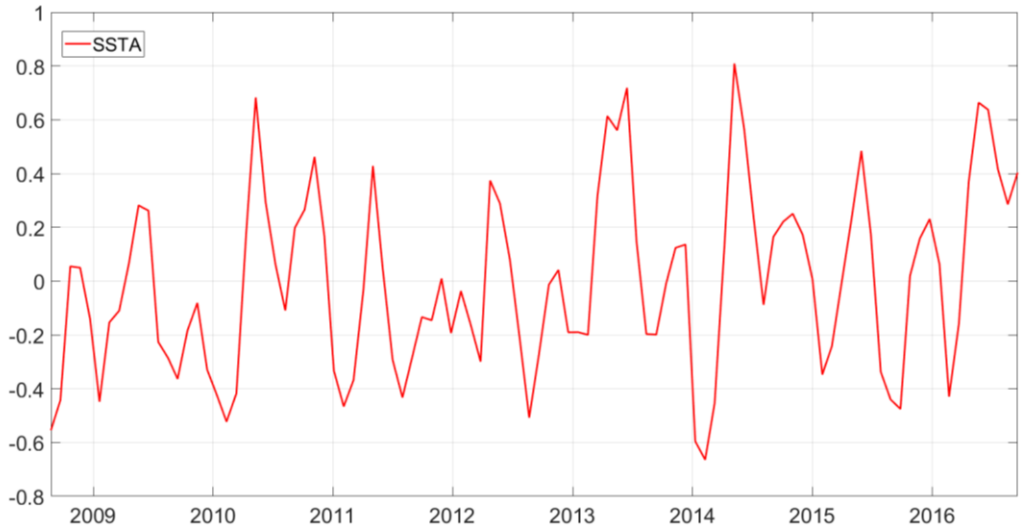

b

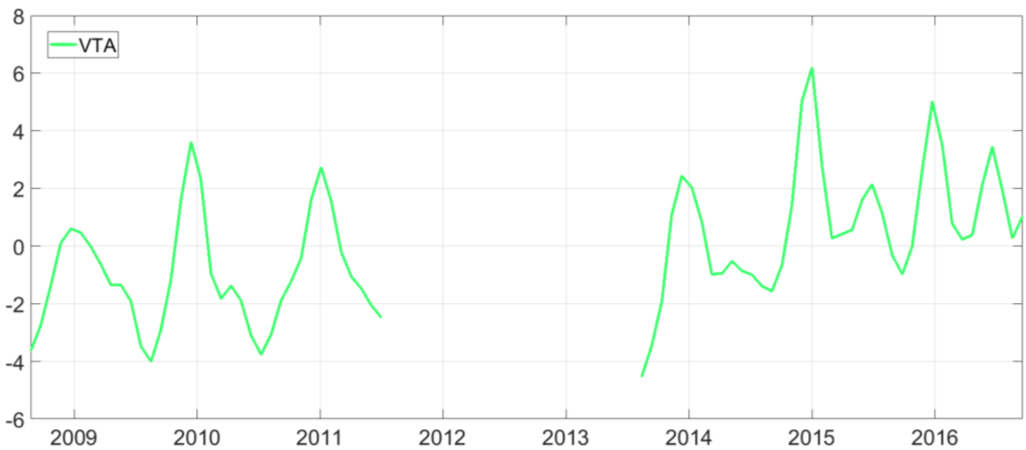

c

Fig.2.2 Time series of SSHA (a), SSTA (b), VTA (c).

2.2.3 Moving average processing

Through Fig.2.2, we will find that the original time series, especially SSHA, are very noisy. And noisy data will have a negative impact on subsequent research. In order to eliminate the effect of short-term changes on the results, the original data of SSH, SST and VT used were smoothed for 90 days (9 cycles). Fig.2.3 shows the time series figures of SSHA, SSTA and VTA after smoothing.

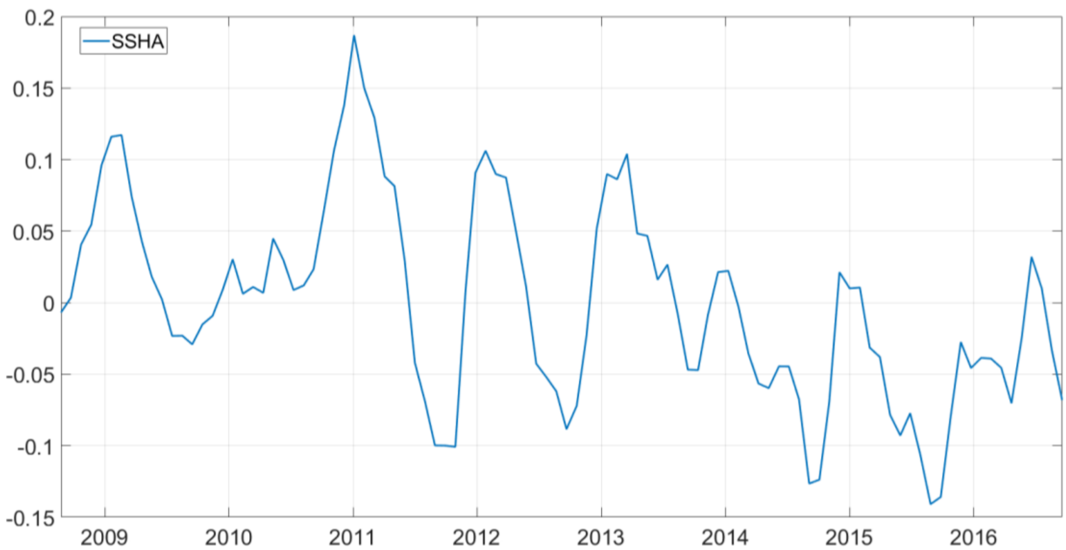

a

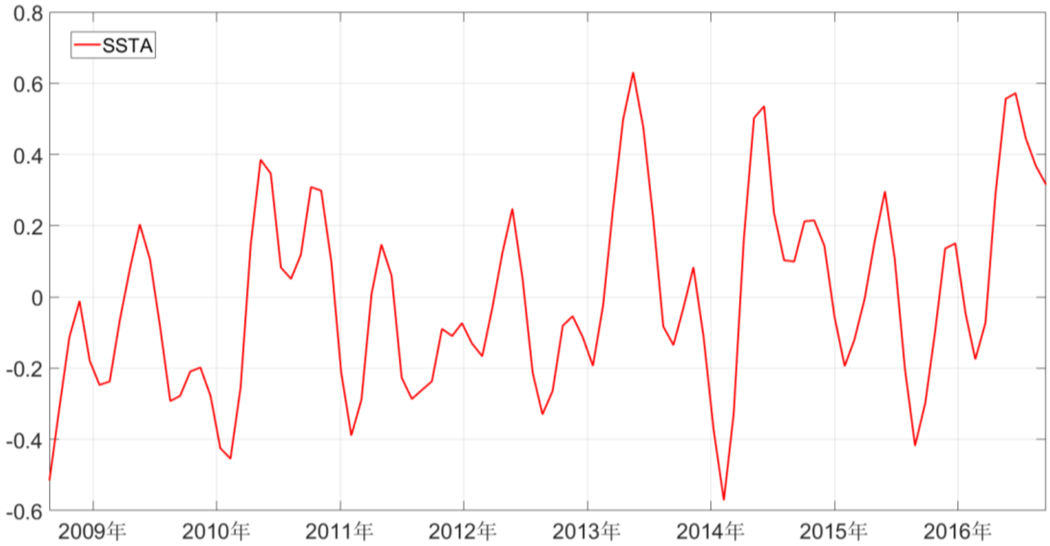

b

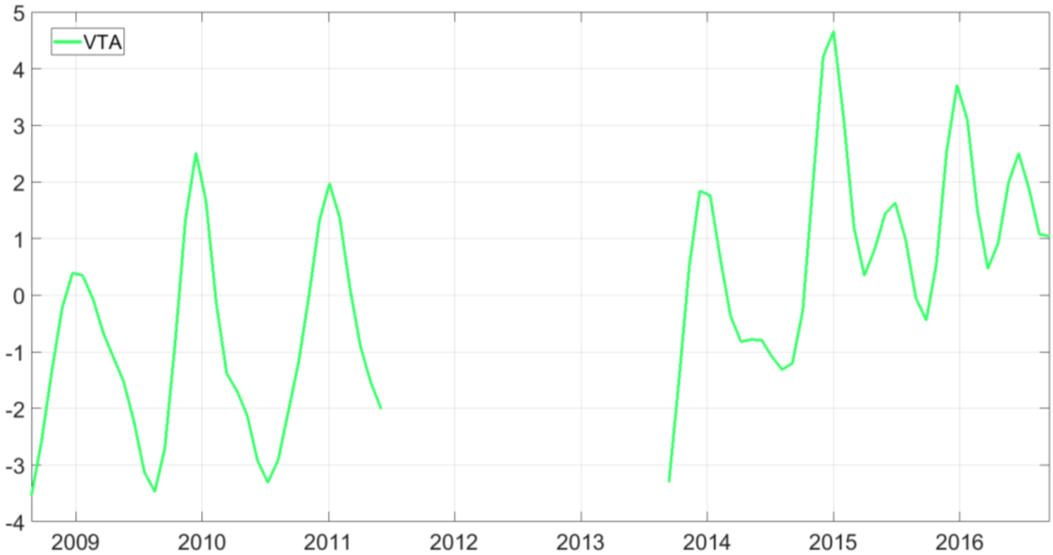

c

Fig.2.3 Time series of SSHA (a), SSTA(b), VTA (c) after smoothing.

2.2.4 Normalized calculation

Because the unit of SSHA data is meter, the unit of SSTA data is degC, and the unit of VTA data is SV. In order to compare SSHA, SSTA and VTA more intuitively and eliminate the influence caused by unit and scale differences among variables, this paper uses normalization to put SSHA, SSTA and VTA into the same dimension for subsequent research.

The calculation of normalization is as follows:

For those with mean value μ and standard deviation σ. The Z value of value X is:

$$z = \frac{(x - \mu)}{\sigma}$$

Z value is measured by standard deviation. The mean value of the standardized data set is 0, the standard deviation is 1, and the shape attributes (the same skewness and kurtosis) of the original data set are retained.

From this, we can get the normalized time series figure of SSHA, SSTA and VTA (Fig.2.4). Please note that the time series of VTA was in a gap from 2011 to 2013.

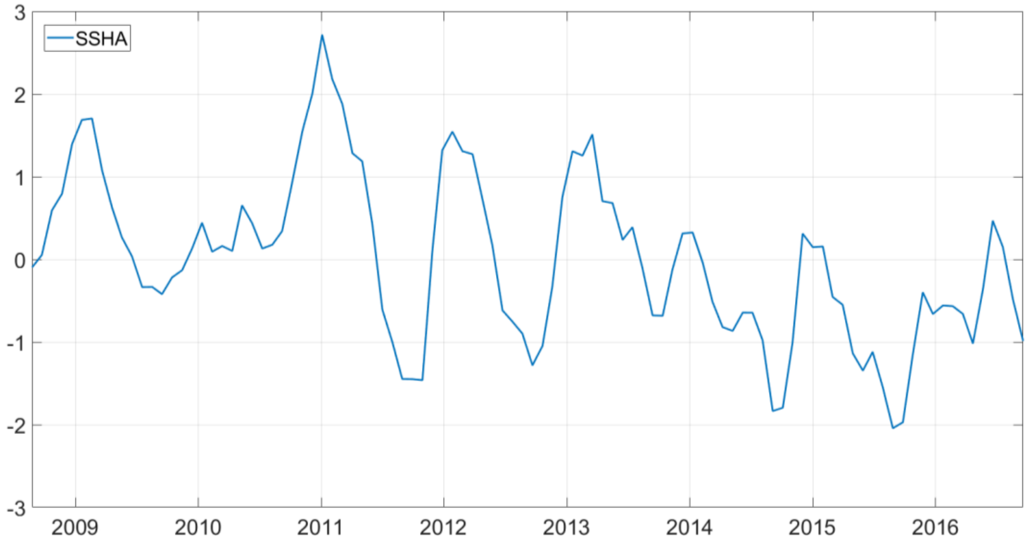
SSHA
3
2
1
0
-1
-2
-3
2009
2010
2011
2012
2013
2014
2015
2016

a

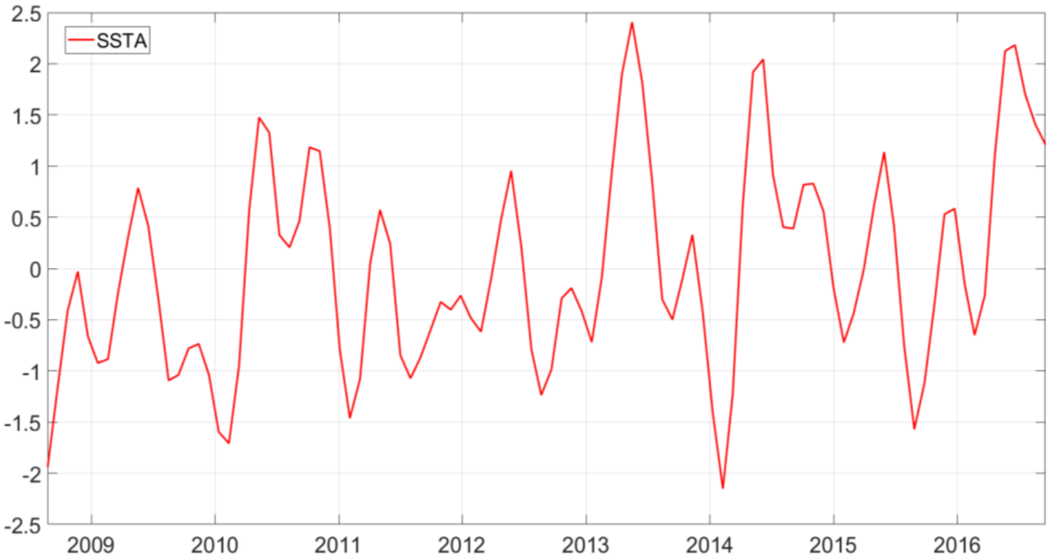
SSTA
2.5
2
1.5
1
0.5
0
-0.5
-1
-1.5
-2
-2.5
2009
2010
2011
2012
2013
2014
2015
2016

b

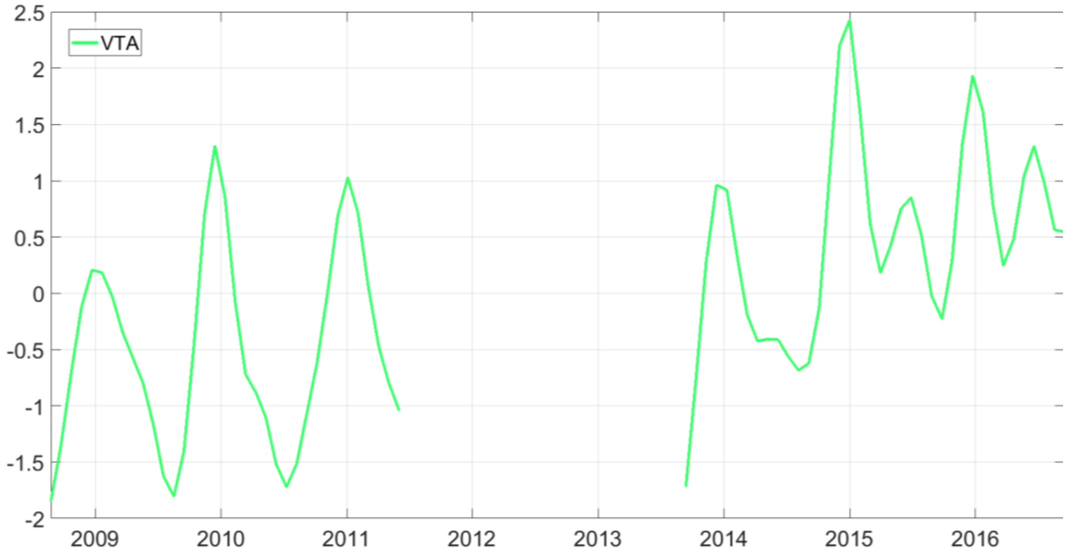

c

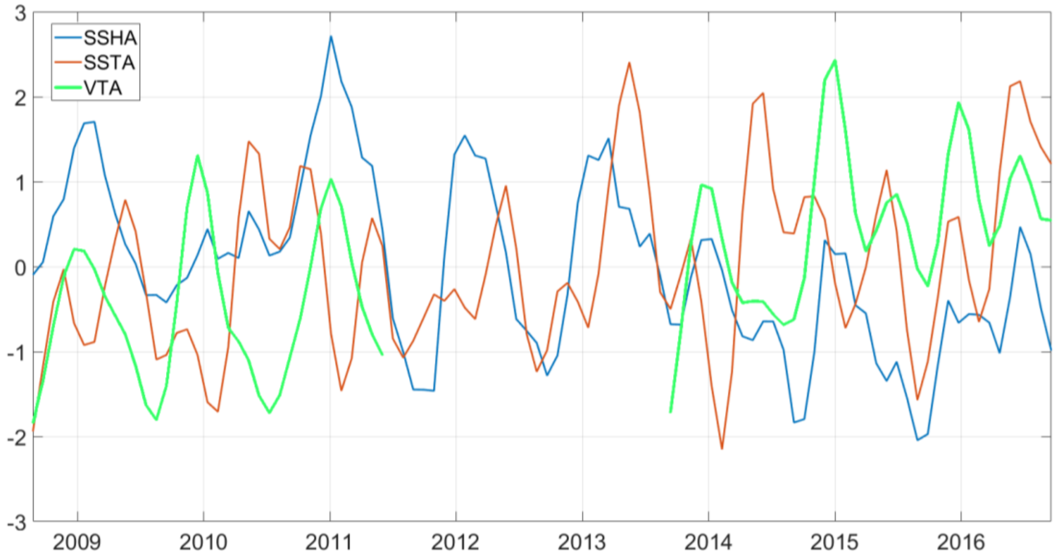

d

Fig.2.4 Time series of normalized SSHA (a), SSTA (b), VTA (c) and combination (d).

2.3 Methods

Through the normalized combination of SSHA, SSTA and VTA time series (Fig. 2.4d), we can see that SSHA, SSTA and VTA are not simple monotonic positive / negative relationship in time series. They have their own characteristics in different periods or seasons. For example, the peak of SSHA always appears at the beginning of 2011-2013, and its trough always appears in the middle of the year. In addition, the climate anomaly ENSO / IOD will also be fed back in the changes of SSHA, SSTA and VTA.

This paper introduces the concept of annual circulation average. Get the average across different years. For example, we use the January data of each year from 2008 to 2016 to extract the average value and obtain it as annual-cycle-mean January data. Based on the results of the annual-cycle-mean, we will further discuss the relationship between SSHA and SSTA.

Because we know that the changes of SSHA and SSTA are complex, we can't study the relationship between SSHA and SSTA by simple seasonal cycle. Therefore, we use the method of sub-seasonal calculation: remove the anomaly from the annual-cycle-mean and get the data of sub-seasonal (anomaly from seasonal cycle) for further study. In order to eliminate the impact of long-term variations in SSHA on the results, we removed 36 months of long-term changes.

3. Results

3.1 Annual-cycle-mean.

3.1.1 For SSHA and VTA

By comparing the sea level difference and Indian Ocean flux (Fig.1.2), Pujina et al. (2019) concluded that the sea level difference in the Strait is controlled by ηS (the SSH in Indian Ocean). This conclusion also provides a certain reference for us to verify our results in annual-cycle-mean SSHA and VTA.

Through compare the time series of annual-cycle-mean SSHA and VTA (Fig. 3.2), we find that SSHA and VTA are in a phase. This means that there is a correlation between SSHA and VTA in annual-cycle-mean.

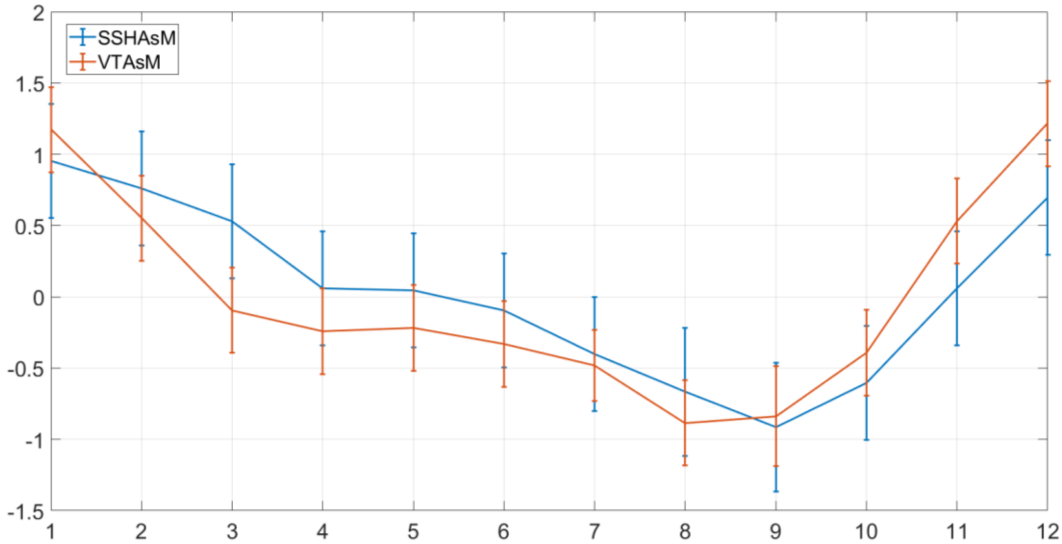

Fig.3.1 Time series of annual-cycle-mean for SSHA and VTA.

For further study and make the results more intuitive, we use the scatter figure for comparison. From the scatter figure (Fig.3.2), we can conclude that SSH tends to synchronize with the Indian Ocean (south of the Strait) in Makassar Strait. This conclusion is consistent with Pujina et al. (2019) study.

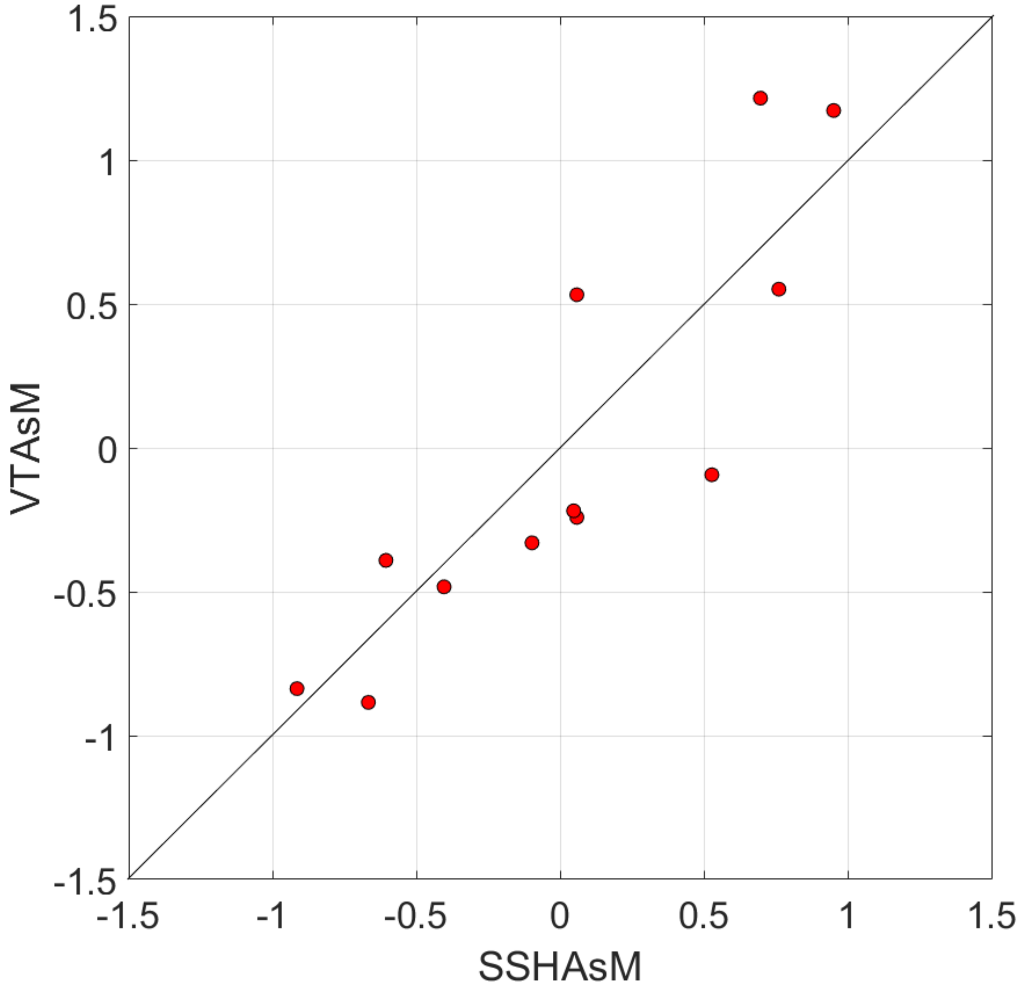

Fig.3.2 Scatter figure for SSHA and VTA in annual-cycle-mean.

3.1.2 For SSHA and SSTA

By observing the time series of annual-cycle-mean SSHA and SSTA (Fig.3.3), we can find that although there is a certain correlation between SSHA and SSTA in a few months. But overall, the annual-cycle-mean of SSHA and SSTA is still out of phase.

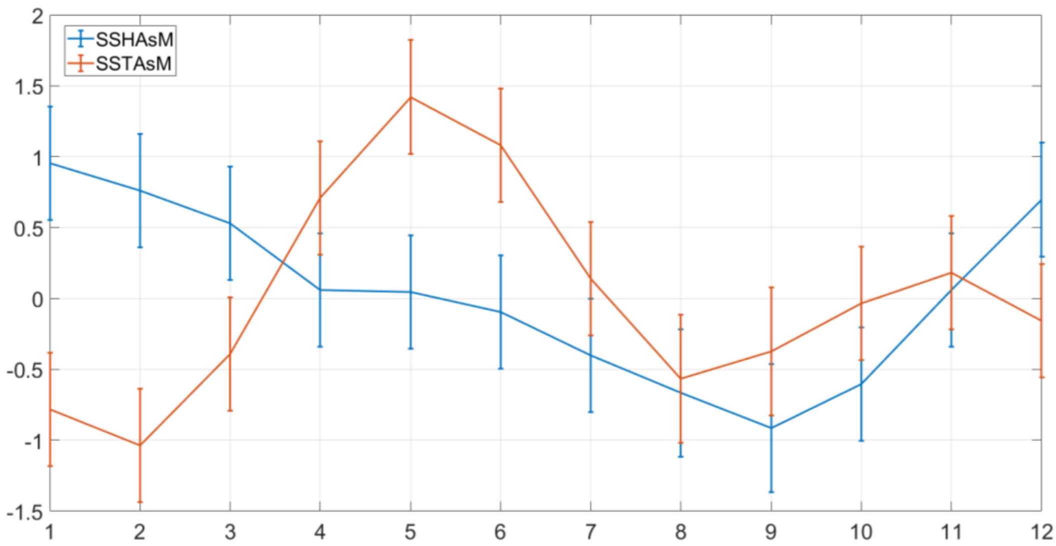

Fig.3.3 Time series of annual-cycle-mean for SSHA and SSTA.

Further study we made the scatter plot of SSHA and SSTA (Fig.3.4). We can find that there are some months' points are separated. The relationship between annual-cycle-mean SSHA and SSTA is not simply. It will mean SSH is not simply related to simply surface heat content.

Combined with the result of annual-cycle-mean figures of SSHA and VTA, as well as the result of annual-cycle-mean figures of SSTA and SSHA. We can get a phased conclusion: for the annual cycle, SSH is related to the pressure difference, rather than simply surface heat content.

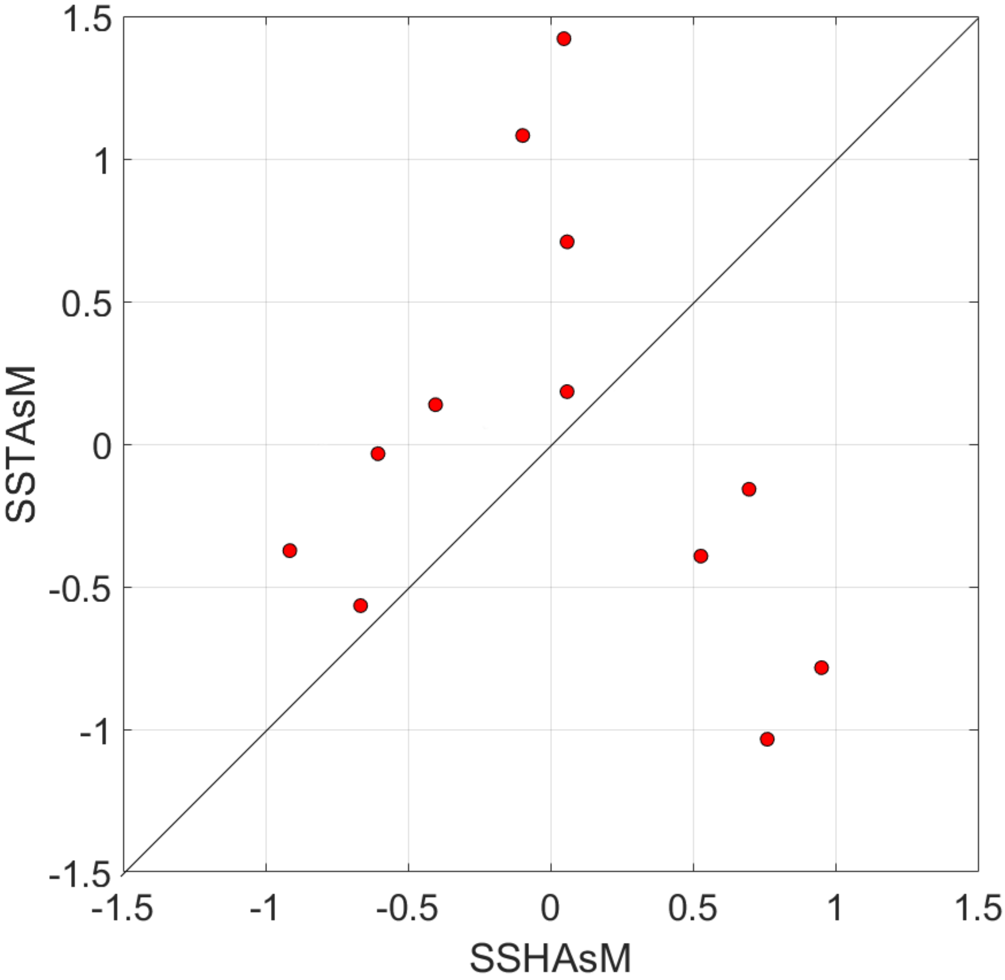

Fig.3.4 Scatter figure for SSHA and SSTA in annual-cycle-mean.

3.2 Sub-seasonal study

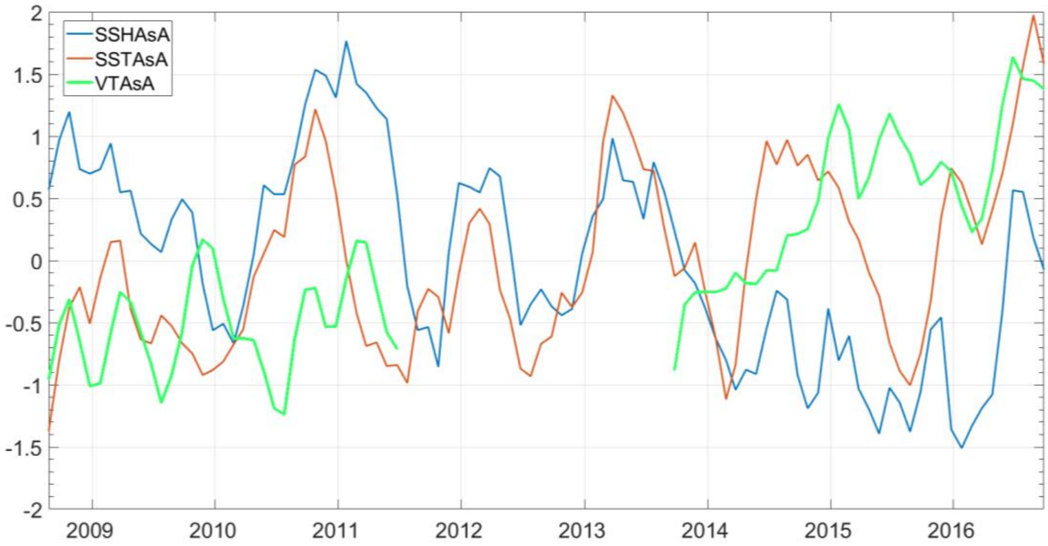

Fig.3.5 Time series of sub-seasonal SSHA, SSTA, VTA.

We remove the anomaly from annual-cycle-mean and get the sub-seasonal data. Through the time series figure of sub-seasonal (Fig.3.5), we can find that there is a significant correlation between the sub-seasonal changes of SSHA and SSTA in some years, or in some time period (like seasons).

We also found that in the time series (Figure 3.5), the maximum and minimum peaks of sub-seasonal SSHA and SSTA often occur at the beginning / middle of the year. We think that this is because the Makassar Strait is mainly dominated by annual variation (monsoon), and the difference between dry and wet seasons is related to the interannual climate event ENSO / IOD. Therefore, we will further study and discuss the relationship between the wet season and the dry season respectively.

We found that in the time series (Fig.3.6), the maximum and minimum peaks of SSHA and SSTA in the sub-seasonal are similar. However, there seems to be a longer-term change in the SSHA in the sub-seasonal, especially in dry season. In order to eliminate the impact of long-term variations in SSHA on the results, we removed 36 months of long-term changes. In the below we show the original sub-seasonal SSHA, 36-month smoothed sub-seasonal SSHA, and the sub-seasonal SSHA after removing the 36-month long-term variations.

Please note that due to the limitation of data length, we may lose the data of the first and last 18 months in 36-month smoothing. In our calculation, when there are not enough elements to fill the window, the window will automatically truncate at the endpoint to calculate the average value. This can explain why the agreement between sub-seasonal SSHA and SSTA is better in the medium term and worse in the initial stage (before the end of 2009) and the end stage (after 2015).

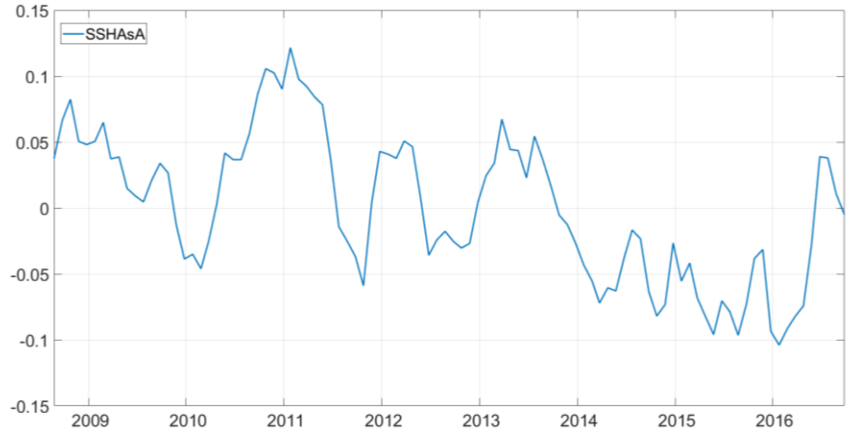

a

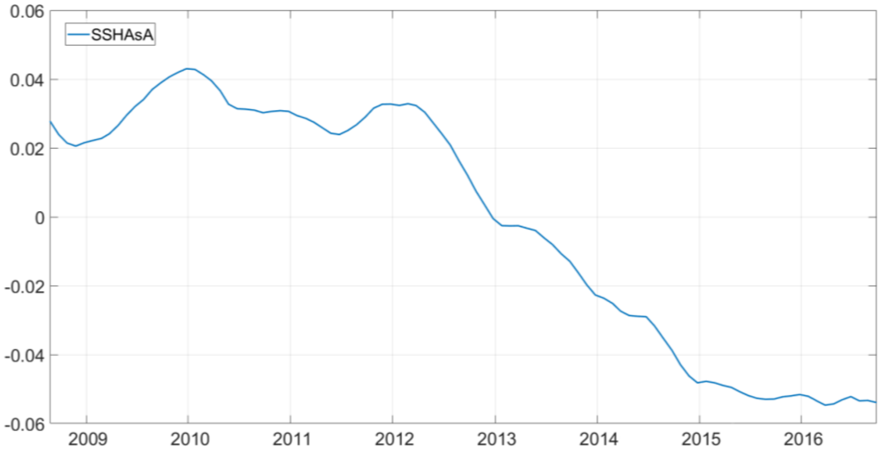

b

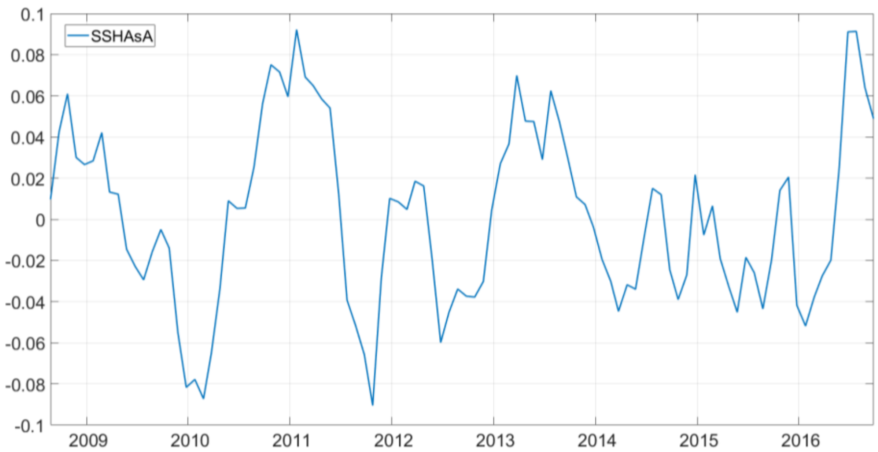

c

Fig.3.6 Time series of original sub-seasonal SSHA (a).
Time series of 36-month smoothed sub-seasonal SSHA (b).
Time series of 36-month-removed sub-seasonal SSHA (c).

3.2.1 Wet season

According to the climate of the study area, we classified December, January, February and March as wet seasons. We used sub-seasonal SSHA and sub-seasonal SSTA wet season data to make a scatter figure (Fig.3.7).

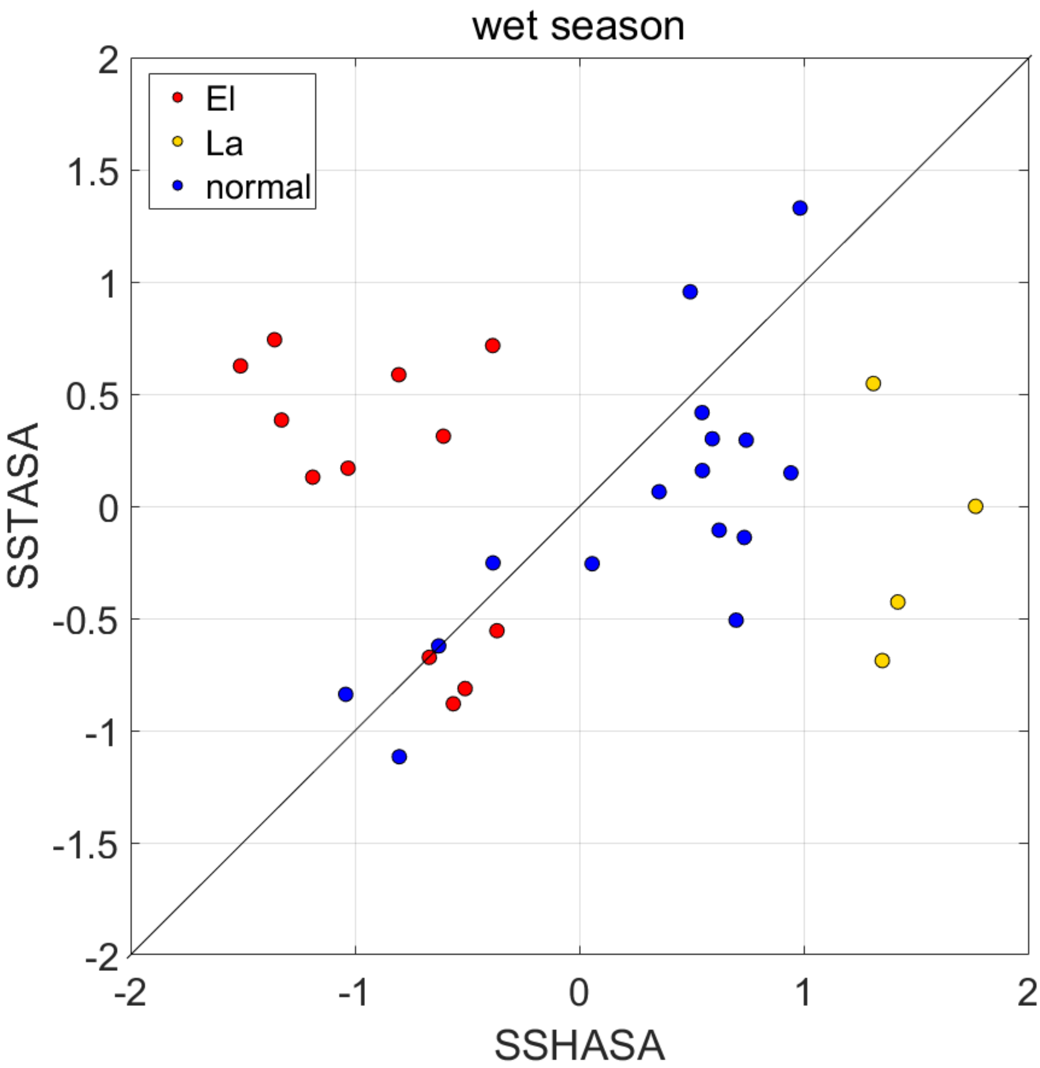

Fig.3.7 Scatter figure for sub-seasonal SSHA and SSTA in El Nino/La Nina/normal.

Through the scatter plot of wet season, we can find that there is a significant positive correlation between SSHA and SSTA in most years (blue dots). It means that sub-seasonal SSHA is related to the surface heat content.

But there are still some outliers. Through the scatter figure we found these outliers are El Nino and La Nina years (red and yellow dots), well the El Nino data of 2009-2010 is still in the same relationship with most years. It means most of ENSO will affect the relationship between sub-seasonal SSHA and SSTA in wet season.

Through the scatter figures of wet season, we can get the periodic conclusion:

1. The variation of sub-seasonal SSHA is related to the surface heat content.

2. The change of surface thickness caused by ENSO will affect the correlation.

3.2.2 Dry season

Similar with wet season, according to the climate of the study area, we classified June, July, August and September as dry season.

It should be noted that in the dry season, we also need to consider the impact of IOD not only for ENSO. Because IOD is only related to the monsoon itself, so we can only discuss the influence of IOD in the dry season.

Since the sub-seasonal SSHA removes the long-term changes of 36 months, we can get clear results between the sub-seasonal SSHA and SSTA. In the “Discussion” Section later, we will discuss the impact of 36-month-removed on the results. And we will show how the results would change if we do not use 36-month- removed.

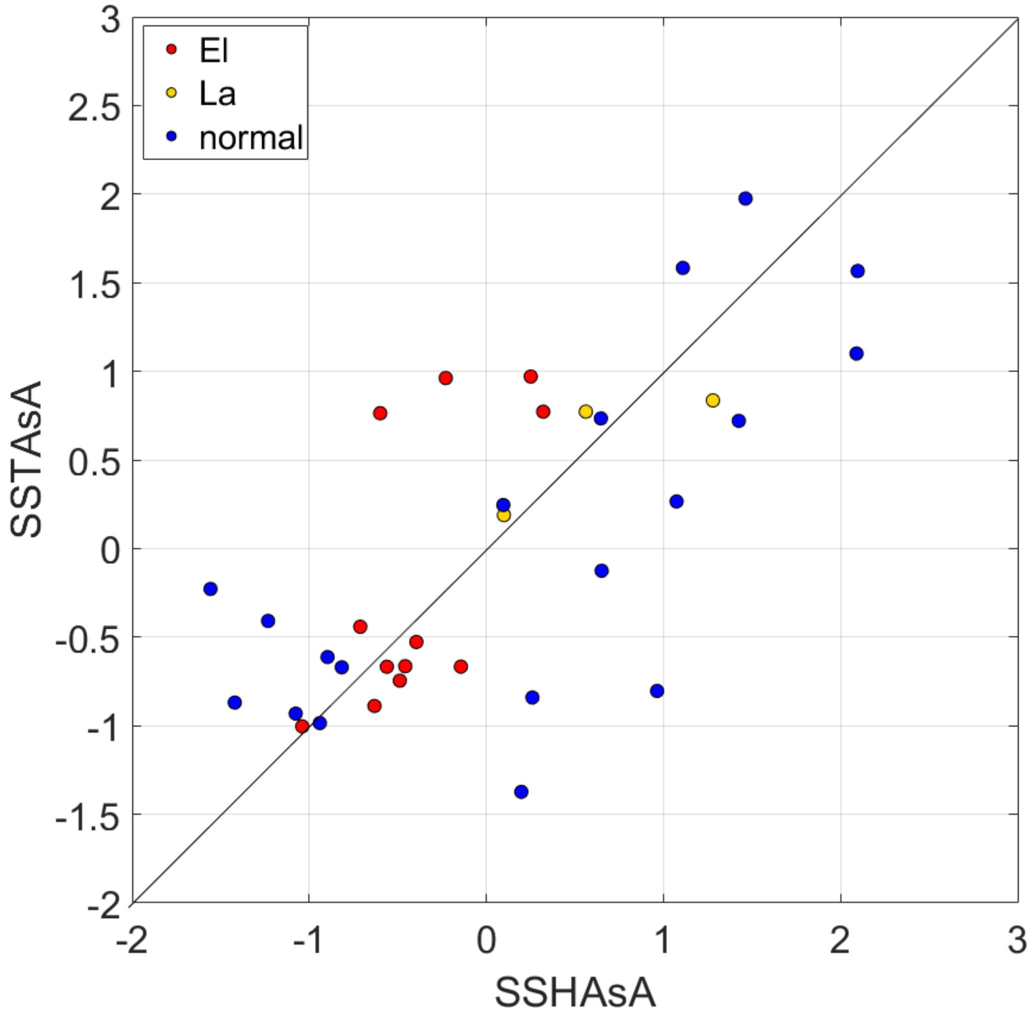

Fig.3.8 Scatter figure for sub-seasonal SSHA with 36-month-removed and SSTA in El Nino/La Nina/normal.

Through the dry season scatter figure in ENSO, we found that there was a significant positive correlation between SSHA and SSTA in the dry season. It seems that this positive correlation is not affected by El Nino or La Nina as ENSO, and the positive correlation is even stronger in La Nina period (CC = 0.84).

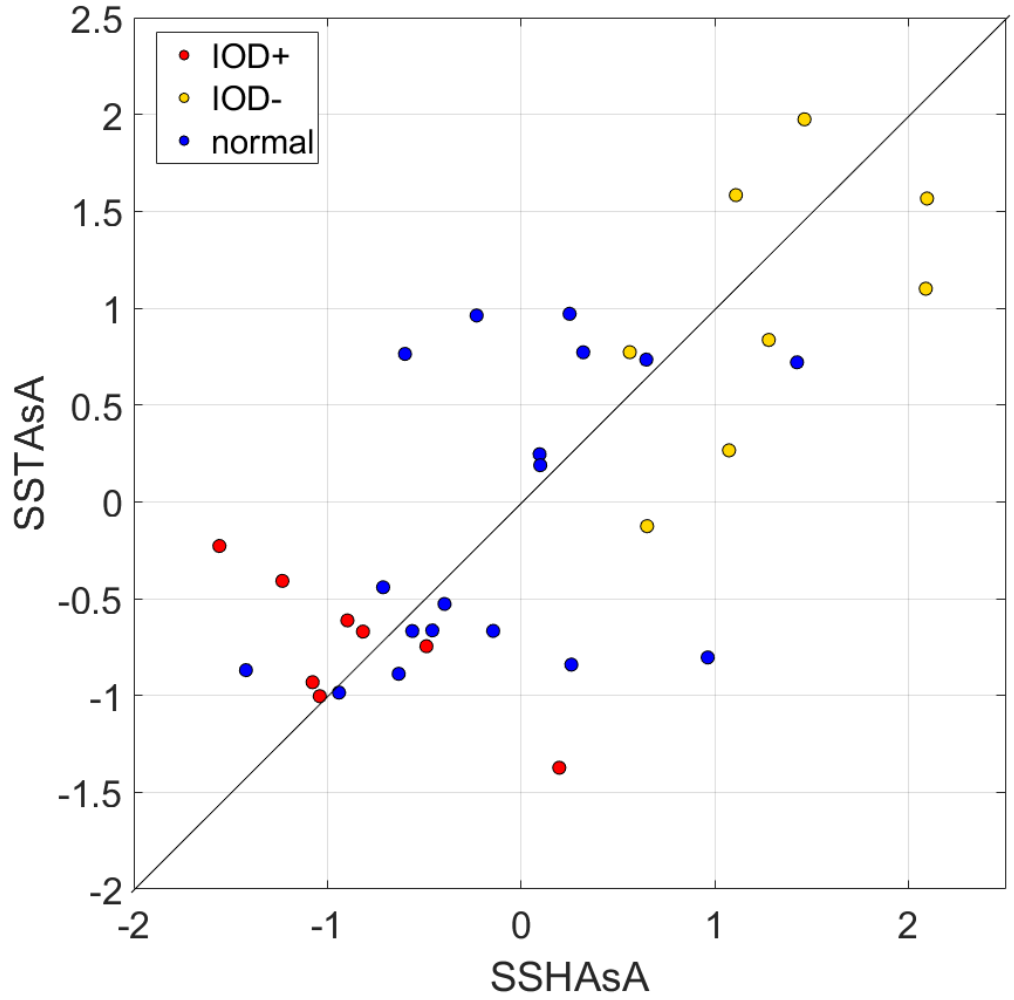

Fig.3.9 Scatter figure for sub-seasonal SSHA with 36-month-removed and SSTA in IOD.

In the period of IOD, positive IOD and negative IOD showed two different results:

In the period of positive IOD, there was a significant negative correlation between SSHA and SSTA in the sub-seasonal (CC = - 0.80), and sub-seasonal SSTA range of positive IDO is smaller than negative IOD /

normal. This is also consistent with the characteristics of abnormal cooling of the coastal waters of the tropical southeast Indian Ocean during the positive phase IOD. However, in the period of negative IOD, there is a positive correlation between SSHA and SSTA in the sub-seasonal (CC = 0.57), which is similarly to that in most years. And the range for SSTA of negative IOD is wider.

Since the Makassar Strait is mainly dominated by annual variation (monsoon), and the difference between dry and wet seasons is related to the interannual climate event ENSO / IOD. Based on the study of sub-seasonal SSHA and SSTA in wet season and dry season, we get the periodic conclusion that in Makassar Strait: the variation of sub-seasonal SSHA and SSTA are related, and the overall correlation is positive.

4. Discussion

4.1 Dependency on temporal smoothing parameters

In Section 3.2.2, we used the sub-seasonal SSHA data with 36-month smoothing removed. Because we found that SSHA and SSTA had similar maximum / minimum peaks in the original sub-seasonal data, but SSHA seemed to have a longer-term change, especially in the dry season. We think that such a long-term change will have a negative impact on the research results.

So, if we do not use 36-month-removed sub-seasonal SSHA, but use the original sub-seasonal SSHA for study, what will be the negative impact? We show the result when we used the sub-seasonal SSHA data without using 36-month- removed to study the dry season with sub-seasonal SSTA, we can get Fig. 4.1.

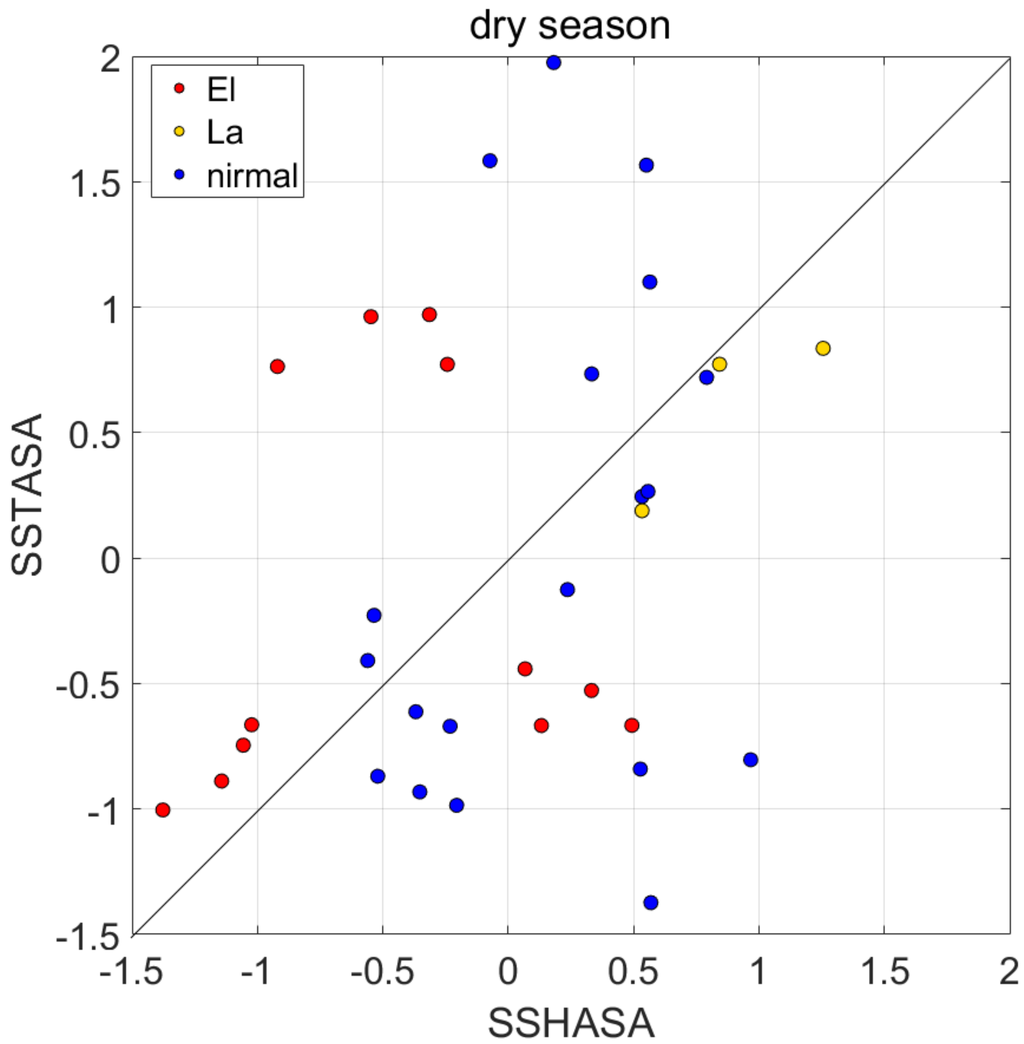

dry season
El
La
nirmal
2
1.5
1
0.5
0
-0.5
-1
-1.5
SSTASA
-1.5
-1
-0.5
0
0.5
1
1.5
2
SSHASA

a

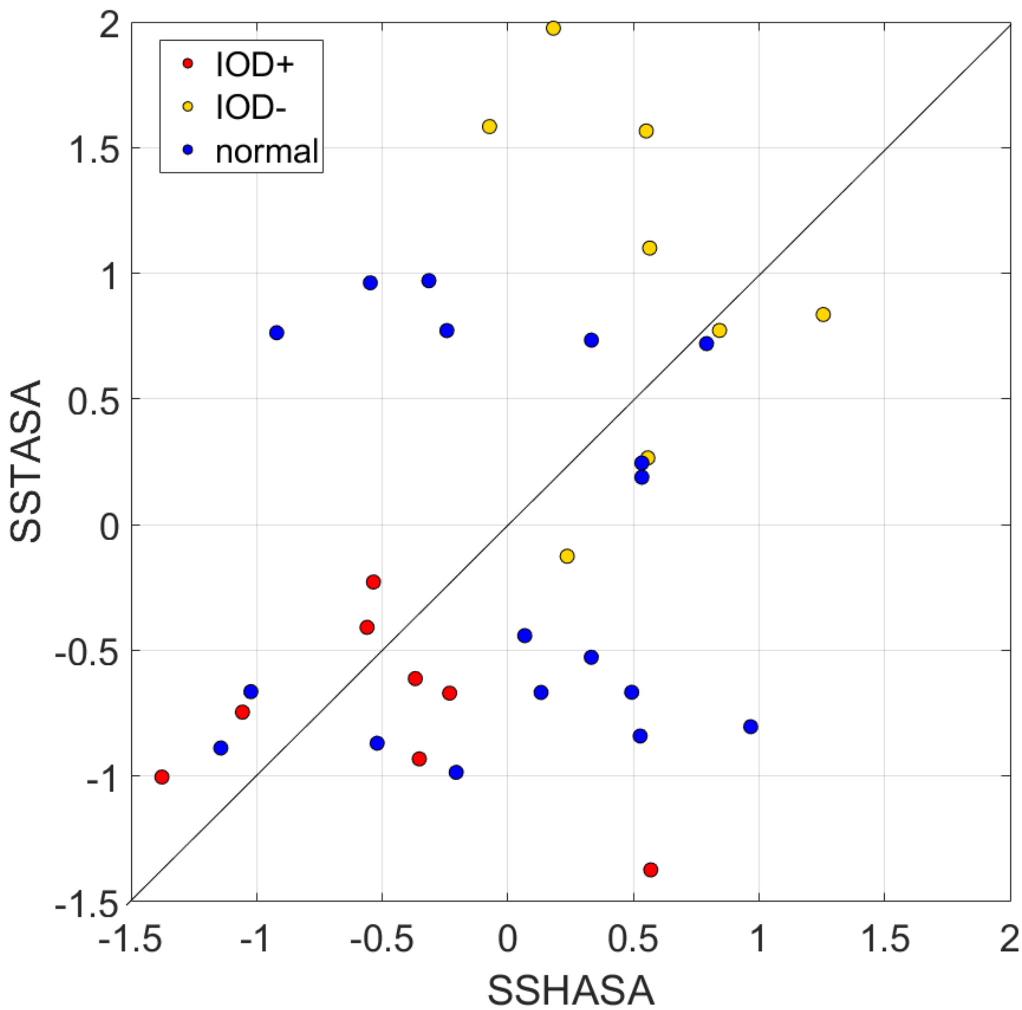

b

Fig.4.1 Scatter figure for sub-seasonal SSHA and SSTA without 36-month-removed in El Nino/La Nina/normal (a) and IOD (b) in dry season.

Through the scatter plot of Fig.4.1, we will find that due to the influence of long-term changes, there is no obvious relationship between SSHA and SSTA in the sub-seasonal of dry season. This result proves the necessity of using 36-month-removed to remove long-term changes.

4.2 Propagations of sub-seasonal variations

Radjawane and Azminuddin (2016) have used altimetry data to focus on sub-seasonal variations in Makassar Strait. They found some variations seemed to propagate from south to north, showed that propagation speed of variations in 2010 has 0.16m/s, which is consistent with Kelvin waves.

Whether in the northern or southern hemisphere, Kelvin waves propagate from the western boundary of the basin to the north and from the eastern boundary to the polar region. The function of the equator is similarly to the terrain boundary of the northern and southern hemispheres, so that Kelvin waves can propagate along the equator. The eastward propagating equatorial Kelvin wave "strikes" the boundary of the basin, part of the energy is reflected in the form of planetary wave or gravity wave, and the rest is transmitted to the poles in the form of Kelvin wave.

Near the equator, the westerly wind burst will push the warm water to the middle of the Pacific Ocean, and the weakened trade wind will make the sea water accumulated in the equatorial western Pacific incline to the East, resulting in Kelvin wave.

Radjawane and Azmiuddin (2016) suggested that is Kelvin wave, but resolution of altimetry data is low (only few occasional tracks within straits). So we have not yet determined that sub-seasonal variations are Kelvin waves.

However, spatial and temporal resolution of altimetry data are low. Since sub-seasonal SSHA and SSTA are revealed in this study well correlated, it is possible to use high-resolution sub-seasonal SSTA data to study propagation of sub-seasonal variations in Makassar Strait.

Meanwhile, we use the Hovmoller diagrams to study the propagation of Kelvin wave in Makassar Strait. Due to the physical properties of Kelvin waves, we will discuss the meridional propagation and the latitudinal propagation in the Strait respectively.

We take the mid-SST in the middle of the Strait as an example to make relevant mapping, and Fig. 4.4 shows the location of west（1°S,117°E）/ mid （1°S,118°E）/ east（1°S,119°E） in the middle of the Strait.

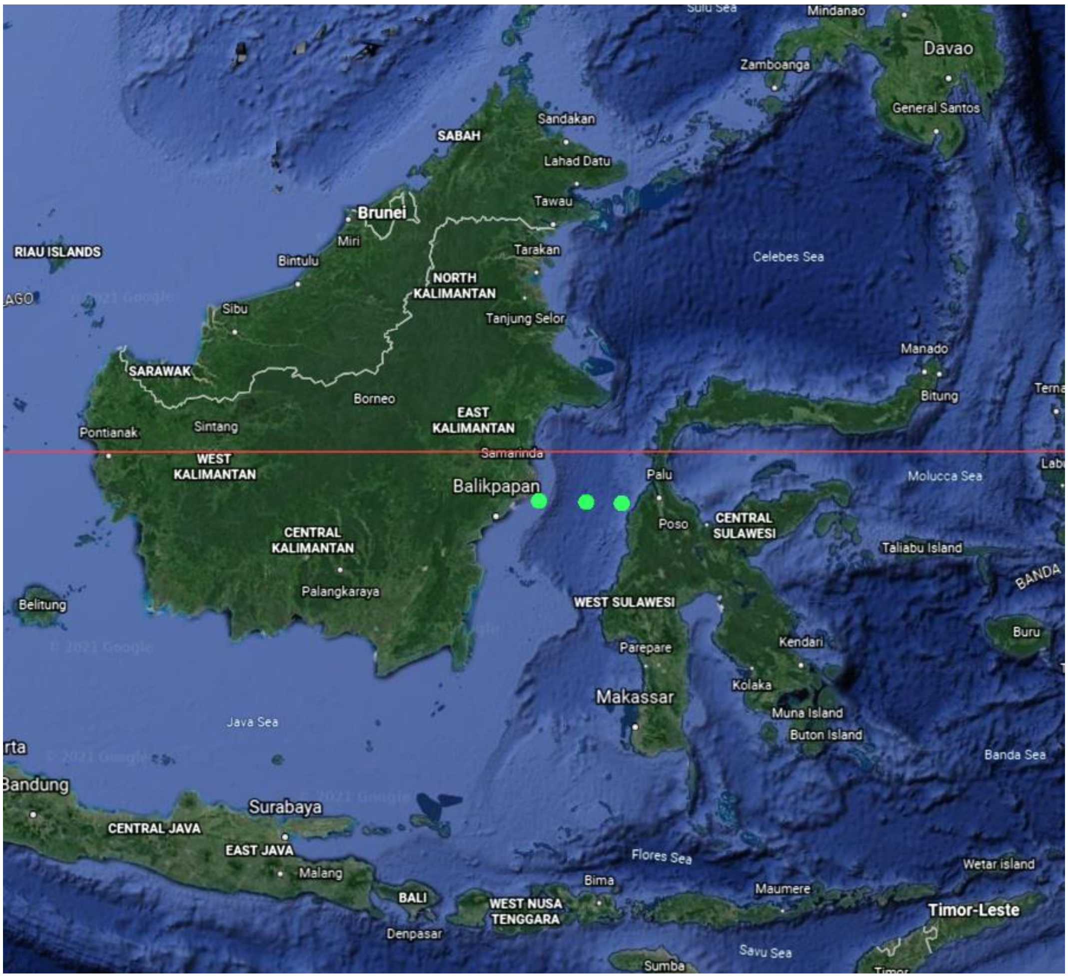

Fig.4.4 Location of west / mid / east in the mid-SST.
(Map source: Google Earth, 2021)

Through the Hovmoller diagram (Fig.4.5), we can see that the SST on the west side of the Strait is always stronger. We found that the negative signal of SST was stronger in the dry season of 2009, 2011, 2012 and 2015. These time periods are similarly to the periods of El Nino and positive IOD. This may be because El Nino and positive IOD will weaken the propagation of sub-seasonal variations.

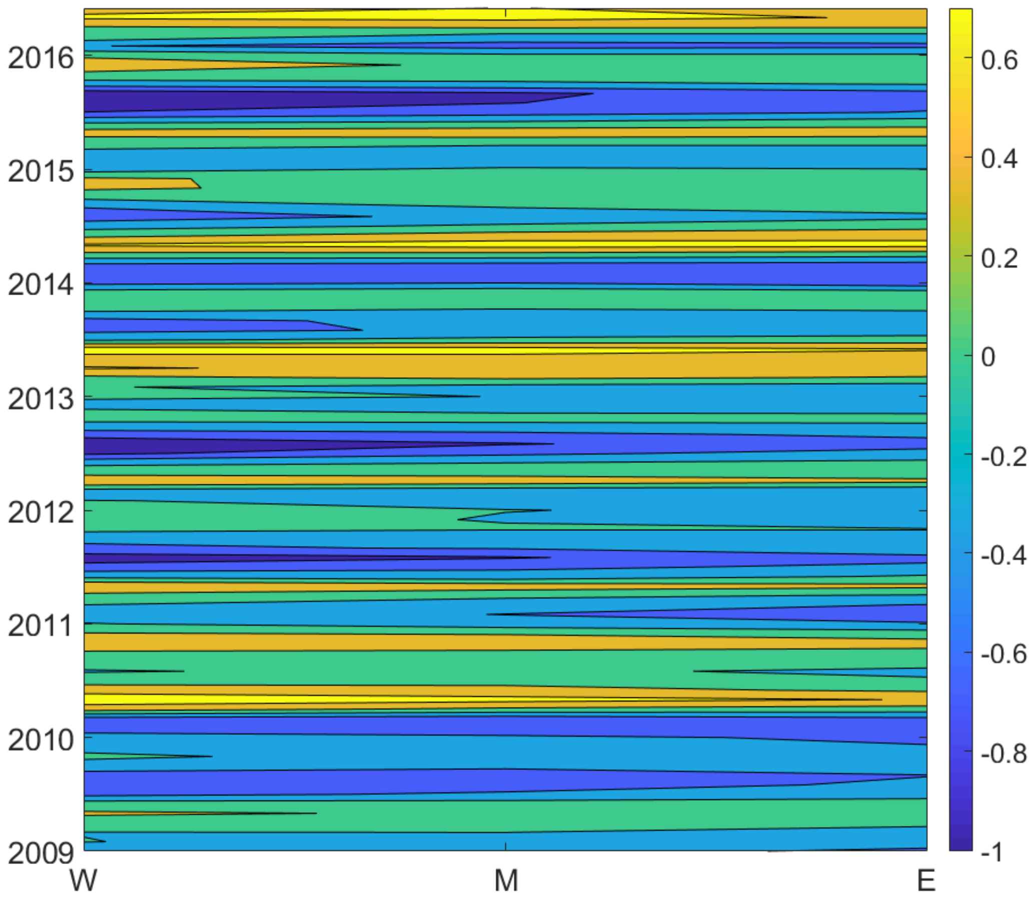

Fig.4.5 Hovmoller diagram for west to east in the mid-SST.

Fig.4.6 shows the SST locations in the west and east of the Strait we used to produce the Hovmoller diagram. For west side are 2°N,118°E / 1°S,117°E / 4°S,116°E ; for east side are 2°N,120°E / 1°S,119°E / 4°S,119°E.

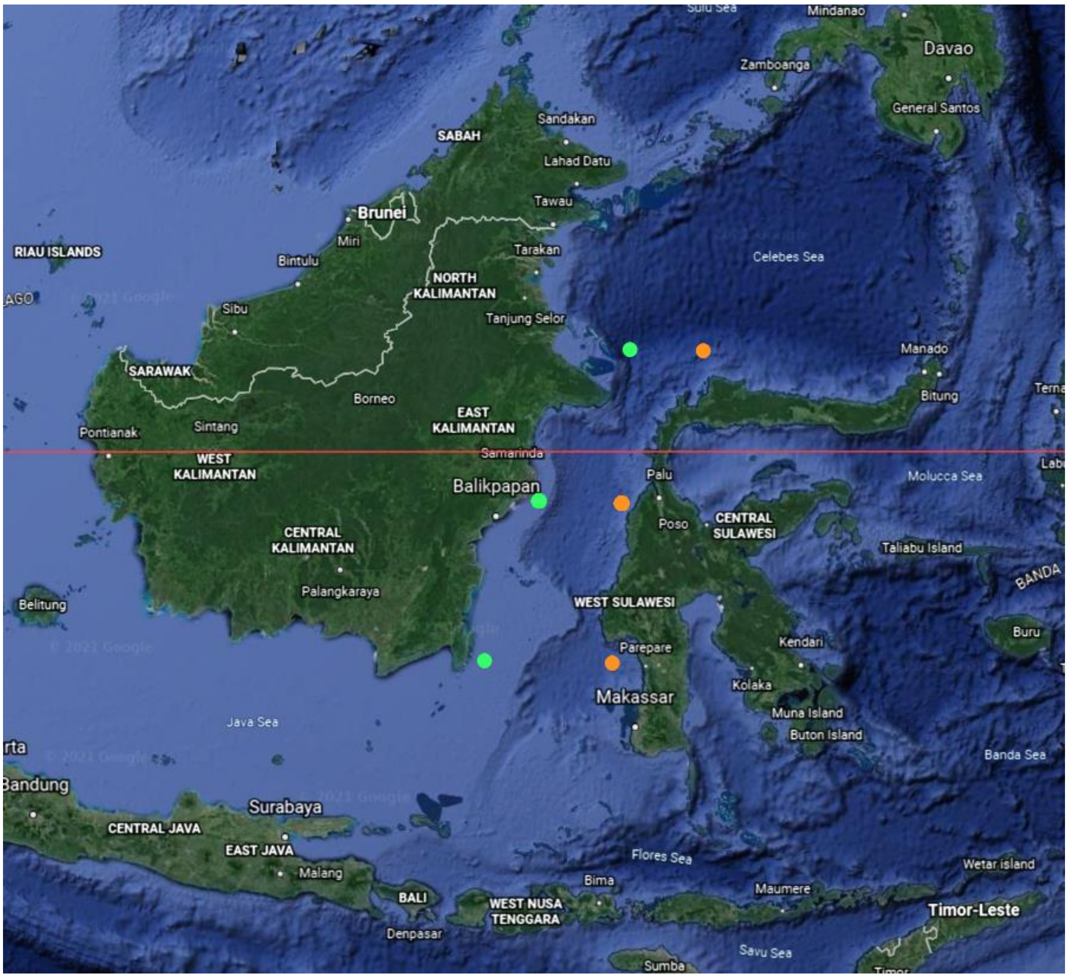

Fig.4.6 Location of west (green) / east (yellow) side in the mid-SST.
(Map source: Google Earth, 2021）

Through the Fig.4.7, we find that: on the east side of the Strait, the clear propagation along the South-North length is not obvious; The strongest signal we found in the south of the Strait did not enter the middle of the Strait. However, on the west side of the Strait, we can find that the signal propagates from the south to the middle and then to the north. We can find some signals show clear northward propagation. Such as positive anomaly in 2010, which is consistent with Radjawane and Azminuddin (2016).

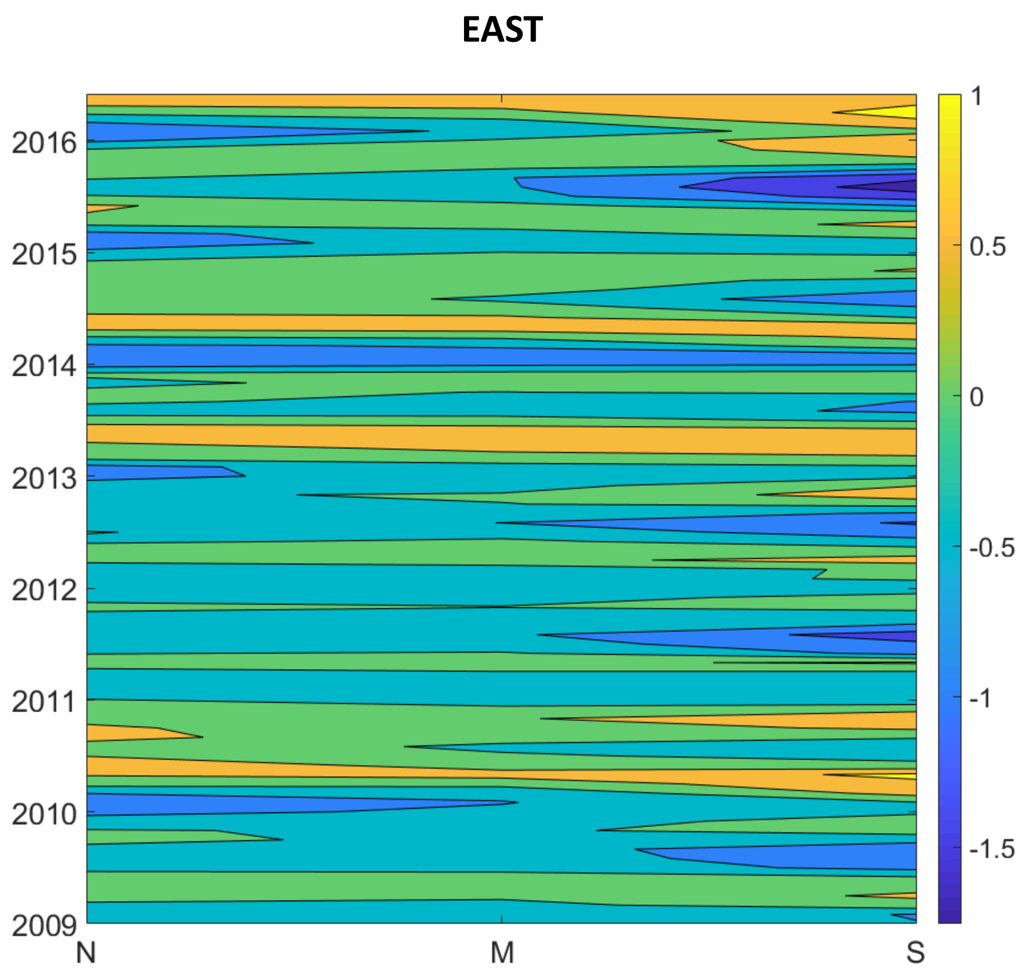

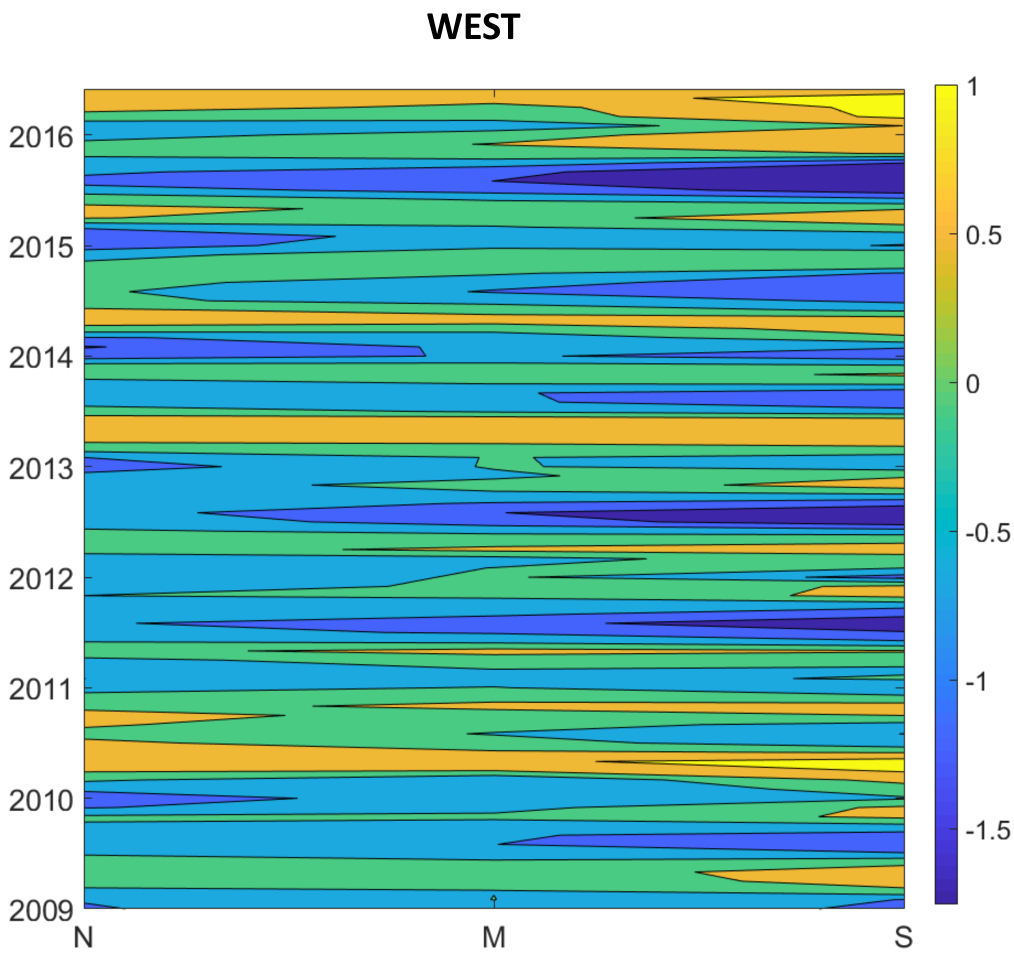

Fig.4.7 Hovmoller diagrams for eastside and westside in the Strait.

Combined with the figures, we can know that in the Makassar Strait, SST anomaly propagates from the south side of the Strait, and the amplitude is stronger in the west side of the Strait. This indicates the possibility of Kelvin wave propagation in the Strait. And we consider that sub-seasonal variations enter the Makassar Strait from the Java Sea (south side of the Makassar Strait), propagate northward along the Strait near the west side, and finally enter the Sulawesi Sea.

5. Conclusion

We use altimetry data within the strait, owing to progress of coastal altimetry data processing. This is also different from the previous study of Pujina et al. (2019) Using SSH in the Pacific and Indian oceans.

In the annual-cycle-mean, the time series of SSHA and VTA are in a phase. This indicates that SSH tends to synchronize with the Indian Ocean in Makassar Strait, and the change of SSH is also related to the pressure difference. The annual cycle of SSHA and SSTA are out of phase, which indicates that SSH is not simply related to the surface heat content.

We get the sub-seasonal data through the anomaly of annual-cycle-mean：

In wet season, there is a significant positive correlation between SSHA and SSTA in most years, and the outliers are El Nino and La Nina years (except 2009-2010 El Nino). We think that the sub-seasonal variation is related to the surface heat content, but the change of surface thickness caused by Enso will affect the correlation.

In the dry season, there is not clearly relationship between SSHA and SSTA in the sub-seasonal. But when we further remove the long-term changes in SSH. There was a significant positive correlation between SSHA and SSTA in most years, especially in La Nina period (CC = 0.84). And sub-seasonal SSTA range of positive IDO is small.

Since sub-seasonal SSHA and SSTA are revealed in this study well correlated, it is possible to use high-resolution sub-seasonal SSTA data to study propagation of sub-seasonal variations in Makassar Strait. By studying the SST in different positions of Makassar Strait, we find that the SST in the west of the Strait is always stronger, and the stronger SST always propagates northward from the south side of the Strait. Therefore, we think that it is possible for Kelvin wave to propagate. And we think the propagation direction of sub-seasonal variations will be: it enters Makassar Strait from Java Sea (south side of Makassar Strait), propagates northward along the Strait near the west side, and finally enters Sulawesi Sea.

6. Reference

Annamalai H, Xie SP, McCreary JP, et al. Impact of Indian Ocean sea surface temperature on developing El Niño. Journal of Climate: 2005, 18(2): 302–319.

Behera SK, Luo JJ, Masson S, et al. A CGCM study on the interaction between IOD and ENSO. Journal of Climate: 2006, 19(9): 1,688–1,705.

Bjerknes J. Atmospheric teleconnections from the equatorial Pacific. Monthly weather review: 1969, 97(3): 163–172.

Gordon, A. L., et al. Makassar Strait Throughflow Seasonal and Interannual Variability: An Overview. Journal of Geophysical Research: Oceans: 2019, 124: 3,724–3,736

Hiroyuki Tomita, Tsutomu Hihara, Shin'ichiro Kako, Masahisa Kubota,Kunio Kutsuwada Journal of Oceanography (2019) 75:171-194

Luo JJ, Zhang R, Behera SK, et al. Interaction between El Nino and extreme Indian ocean dipole. Journal of Climate: 2010, 23(3): 726–742.

Mayer, B., and P. E. Damm (2012), The Makassar Strait throughflow and its jet, J. Geophys. Res., 117, C07020, doi:10.1029/2011JC007809.

Napitu A.M., et al. The Madden-Julian Oscillation's Impact on the Makassar Strait Surface Layer Transport. Journal of Geophysical

Research: Oceans: 2019, 124: 3,538–3,550

Pujiana, K., et al. Unprecedented Response of Indonesian Throughflow to Anomalous Indo-Pacific Climatic Forcing in 2016. Journal of Geophysical Research: Oceans: 2019, 124: 3,737–3,754

Radjawane and F Azminuddin. Seasonal and semi-annual variability of sea surface height in Makassar Strait. 2016 J. Phys.: Conf. Ser. 739 012067

Rao RR, Molinari RL, Festa JF. Evolution of the climatological near-surface thermal structure of the tropical Indian Ocean: 1. Description of mean monthly mixed layer depth, and sea surface temperature, surface current, and surface meteorological fields. Journal of Geophysical Research: Oceans: 1989, 94(C8): 10,801–10,815.

Saji N, Goswami BN, Vinayachandran P, et al. A dipole mode in the tropical Indian Ocean. Nature: 1999, 401: 360–363.

Wang C, Xie SP, Carton JA. Earth's climate: the ocean-atmosphere interaction. WashingtonDC American Geophysical Union Geophysical Monograph Series: 2004, 147.

Wang et al. (2019).

7. Acknowledgements

In the course of this study, I have received much guidance, help and support from many people. Here, I would like to extend my sincere gratitude.

I am greatly indebted to my supervisor, Kaoru Ichikawa, Associate Professor of Research Institute for Applied Mechanics of Kyushu University, has made great contributions to the research direction, research methods and suggestions of the paper. Without his guidance, this study is difficult to proceed smoothly. I would like to thank Associate Professor Ichikawa for his education and guidance.

And I also indebted to Ms. Noriko Takata, has provided a lot of help for my study and life in school. My predecessors, Wang Chuanbing, He Yuqing, Dr. Sakai Akira and Dr. Ji Mengran of other majors, have also helped me a lot in my study and life in Japan. As well as Gu Dexin and Li Daxing, who are also G30, we exchanged many suggestions on research and papers.

Finally, I would like to thank my parents and my lovely cat for their spiritual and financial support during my study abroad.